

Observation of the W -Annihilation Decay $D_s^+ \rightarrow \omega\pi^+$ and Evidence for $D_s^+ \rightarrow \omega K^+$

M. Ablikim¹, M. N. Achasov^{10,d}, S. Ahmed¹⁵, M. Albrecht⁴, M. Alekseev^{56A,56C}, A. Amoroso^{56A,56C}, F. F. An¹, Q. An^{53,43}, J. Z. Bai¹, Y. Bai⁴², O. Bakina²⁷, R. Baldini Ferroli^{23A}, Y. Ban³⁵, K. Begzsuren²⁵, J. V. Bennett⁵, N. Berger²⁶, M. Bertani^{23A}, D. Bettoni^{24A}, F. Bianchi^{56A,56C}, E. Boger^{27,b}, I. Boyko²⁷, R. A. Briere⁵, H. Cai⁵⁸, X. Cai^{1,43}, A. Calcaterra^{23A}, G. F. Cao^{1,47}, N. Cao^{1,47}, S. A. Cetin^{46B}, J. Chai^{56C}, J. F. Chang^{1,43}, G. Chelkov^{27,b,c}, G. Chen¹, H. S. Chen^{1,47}, J. C. Chen¹, M. L. Chen^{1,43}, S. J. Chen³³, X. R. Chen³⁰, Y. B. Chen^{1,43}, W. Cheng^{56C}, X. K. Chu³⁵, G. Cibinetto^{24A}, F. Cossio^{56C}, X. F. Cui³⁴, H. L. Dai^{1,43}, J. P. Dai^{38,h}, A. Dbeysi¹⁵, D. Dedovich²⁷, Z. Y. Deng¹, A. Denig²⁶, I. Denysenko²⁷, M. Destefanis^{56A,56C}, F. De Mori^{56A,56C}, Y. Ding³¹, C. Dong³⁴, J. Dong^{1,43}, L. Y. Dong^{1,47}, M. Y. Dong^{1,43,47}, S. X. Du⁶¹, J. Fang^{1,43}, S. S. Fang^{1,47}, Y. Fang¹, R. Farinelli^{24A,24B}, L. Fava^{56B,56C}, F. Feldbauer⁴, G. Felici^{23A}, C. Q. Feng^{53,43}, M. Fritsch⁴, C. D. Fu¹, Q. Gao¹, X. L. Gao^{53,43}, Y. Gao⁴⁵, Y. Gao⁵⁴, Y. G. Gao⁶, Z. Gao^{53,43}, B. Garillon²⁶, I. Garzia^{24A}, A. Gilman⁵⁰, K. Goetzen¹¹, L. Gong³⁴, W. X. Gong^{1,43}, W. Gradl²⁶, M. Greco^{56A,56C}, M. H. Gu^{1,43}, Y. T. Gu¹³, A. Q. Guo¹, R. P. Guo^{1,47}, Y. P. Guo²⁶, A. Guskov²⁷, S. Han⁵⁸, X. Q. Hao¹⁶, F. A. Harris⁴⁸, K. L. He^{1,47}, X. Q. He⁵², F. H. Heinsius⁴, T. Held⁴, Y. K. Heng^{1,43,47}, Y. R. Hou⁴⁷, Z. L. Hou¹, H. M. Hu^{1,47}, J. F. Hu^{38,h}, T. Hu^{1,43,47}, Y. Hu¹, G. S. Huang^{53,43}, J. S. Huang¹⁶, X. T. Huang³⁷, Z. L. Huang³¹, T. Hussain⁵⁵, W. Ikegami Andersson⁵⁷, W. Imoehl²², M. Irshad^{53,43}, Q. Ji¹, Q. P. Ji¹⁶, X. B. Ji^{1,47}, X. L. Ji^{1,43}, X. S. Jiang^{1,43,47}, X. Y. Jiang³⁴, J. B. Jiao³⁷, Z. Jiao¹⁸, D. P. Jin^{1,43,47}, S. Jin^{1,47}, Y. Jin⁴⁹, T. Johansson⁵⁷, N. Kalantar-Nayestanaki²⁹, X. S. Kang³⁴, R. Kappert²⁹, M. Kavatsyuk²⁹, B. C. Ke¹, I. K. Keshk⁴, T. Khan^{53,43}, A. Khoukaz⁵¹, P. Kiese²⁶, R. Kiuchi¹, R. Kliemt¹¹, L. Koch²⁸, O. B. Kolcu^{46B,f}, B. Kopf⁴, M. Kuemmel⁴, M. Kuessner⁴, A. Kupsc⁵⁷, M. Kurth¹, M. G. Kurth^{1,47}, W. Kühn²⁸, J. S. Lange²⁸, P. Larin¹⁵, L. Lavezzi^{56C}, H. Leithof²⁶, C. Li⁵⁷, Cheng Li^{53,43}, D. M. Li⁶¹, F. Li^{1,43}, F. Y. Li³⁵, G. Li¹, H. B. Li^{1,47}, H. J. Li^{1,47}, J. C. Li¹, J. W. Li⁴¹, Jin Li³⁶, K. J. Li⁴⁴, Kang Li¹⁴, Ke Li¹, L. K. Li¹, Lei Li³, P. L. Li^{53,43}, P. R. Li^{47,7}, Q. Y. Li³⁷, W. D. Li^{1,47}, W. G. Li¹, X. L. Li³⁷, X. N. Li^{1,43}, X. Q. Li³⁴, Z. B. Li⁴⁴, H. Liang^{53,43}, H. Liang^{1,47}, Y. F. Liang⁴⁰, Y. T. Liang²⁸, G. R. Liao¹², L. Z. Liao^{1,47}, J. Libby²¹, C. X. Lin⁴⁴, D. X. Lin¹⁵, B. Liu^{38,h}, B. J. Liu¹, C. X. Liu¹, D. Liu^{53,43}, D. Y. Liu^{38,h}, F. H. Liu³⁹, Fang Liu¹, Feng Liu⁶, H. B. Liu¹³, H. M. Liu^{1,47}, Huanhuan Liu¹, Huihui Liu¹⁷, J. B. Liu^{53,43}, J. Y. Liu^{1,47}, K. Y. Liu³¹, Ke Liu⁶, L. D. Liu³⁵, Q. Liu⁴⁷, S. B. Liu^{53,43}, X. Liu³⁰, X. Y. Liu^{1,47}, Y. B. Liu³⁴, Z. A. Liu^{1,43,47}, Zhiqing Liu²⁶, Y. F. Long³⁵, X. C. Lou^{1,43,47}, H. J. Lu¹⁸, J. G. Lu^{1,43}, Y. Lu¹, Y. P. Lu^{1,43}, C. L. Luo³², M. X. Luo⁶⁰, T. Luo^{9,j}, X. L. Luo^{1,43}, S. Lusso^{56C}, X. R. Lyu⁴⁷, F. C. Ma³¹, H. L. Ma¹, L. L. Ma³⁷, M. M. Ma^{1,47}, Q. M. Ma¹, T. Ma¹, X. N. Ma³⁴, X. Y. Ma^{1,43}, Y. M. Ma³⁷, F. E. Maas¹⁵, M. Maggiora^{56A,56C}, S. Maldaner²⁶, Q. A. Malik⁵⁵, A. Mangoni^{23B}, Y. J. Mao³⁵, Z. P. Mao¹, S. Marcello^{56A,56C}, Z. X. Meng⁴⁹, J. G. Messchendorp²⁹, G. Mezzadri^{24B}, J. Min^{1,43}, R. E. Mitchell²², X. H. Mo^{1,43,47}, Y. J. Mo⁶, C. Morales Morales¹⁵, N. Yu. Muchnoi^{10,d}, H. Muramatsu⁵⁰, A. Mustafa⁴, Y. Nefedov²⁷, F. Nerling¹¹, I. B. Nikolaev^{10,d}, Z. Ning^{1,43}, S. Nisar⁸, S. L. Niu^{1,43}, X. Y. Niu^{1,47}, S. L. Olsen^{36,k}, Q. Ouyang^{1,43,47}, S. Pacetti^{23B}, Y. Pan^{53,43}, M. Papenbrock⁵⁷, P. Patteri^{23A}, M. Pelizaeus⁴, J. Pellegrino^{56A,56C}, H. P. Peng^{53,43}, K. Peters^{11,g}, J. Pettersson⁵⁷, J. L. Ping³², R. G. Ping^{1,47}, A. Pitka⁴, R. Poling⁵⁰, V. Prasad^{53,43}, M. Qi³³, T. Y. Qi², S. Qian^{1,43}, C. F. Qiao⁴⁷, N. Qin⁵⁸, X. S. Qin⁴, Z. H. Qin^{1,43}, J. F. Qiu¹, S. Q. Qu³⁴, K. H. Rashid^{55,i}, C. F. Redmer²⁶, M. Richter⁴, M. Ripka²⁶, A. Rivetti^{56C}, V. Rodin²⁹, M. Rolo^{56C}, G. Rong^{1,47}, Ch. Rosner¹⁵, A. Sarantsev^{27,e}, M. Savrié^{24B}, K. Schoenning⁵⁷, W. Shan¹⁹, X. Y. Shan^{53,43}, M. Shao^{53,43}, C. P. Shen², P. X. Shen³⁴, X. Y. Shen^{1,47}, H. Y. Sheng¹, X. Shi^{1,43}, J. J. Song³⁷, X. Y. Song¹, S. Sosio^{56A,56C}, C. Sowa⁴, S. Spataro^{56A,56C}, G. X. Sun¹, J. F. Sun¹⁶, L. Sun⁵⁸, S. S. Sun^{1,47}, X. H. Sun¹, Y. J. Sun^{53,43}, Y. K. Sun^{53,43}, Y. Z. Sun¹, Z. J. Sun^{1,43}, Z. T. Sun²², Y. T. Tan^{53,43}, C. J. Tang⁴⁰, G. Y. Tang¹, X. Tang¹, B. Tsednee²⁵, I. Uman^{46D}, B. Wang¹, D. Wang³⁵, D. Y. Wang³⁵, K. Wang^{1,43}, L. L. Wang¹, L. S. Wang¹, M. Wang³⁷, Meng Wang^{1,47}, P. Wang¹, P. L. Wang¹, W. P. Wang^{53,43}, X. L. Wang^{9,j}, Y. Wang^{53,43}, Y. F. Wang^{1,43,47}, Z. Wang^{1,43}, Z. G. Wang^{1,43}, Z. Y. Wang¹, Zongyuan Wang^{1,47}, T. Weber⁴, D. H. Wei¹², P. Weidenkaff²⁶, S. P. Wen¹, U. Wiedner⁴, M. Wolke⁵⁷, L. H. Wu¹, L. J. Wu^{1,47}, Z. Wu^{1,43}, L. Xia^{53,43}, Y. Xia²⁰, S. Y. Xiao¹, Y. J. Xiao^{1,47}, Z. J. Xiao³², Y. G. Xie^{1,43}, Y. H. Xie⁶, X. A. Xiong^{1,47}, Q. L. Xiu^{1,43}, G. F. Xu¹, J. J. Xu^{1,47}, L. Xu¹, Q. J. Xu¹⁴, X. P. Xu⁴¹, F. Yan⁵⁴, L. Yan^{56A,56C}, W. B. Yan^{53,43}, W. C. Yan², Y. H. Yan²⁰, H. J. Yang^{38,h}, H. X. Yang¹, L. Yang⁵⁸, R. X. Yang^{53,43}, Y. H. Yang³³, Y. X. Yang¹², Yifan Yang^{1,47}, Z. Q. Yang²⁰, M. Ye^{1,43}, M. H. Ye⁷, J. H. Yin¹, Z. Y. You⁴⁴, B. X. Yu^{1,43,47}, C. X. Yu³⁰, J. S. Yu³⁰, J. S. Yu²⁰, C. Z. Yuan^{1,47}, Y. Yuan¹, A. Yuncu^{46B,a}, A. A. Zafar⁵⁵, Y. Zeng²⁰, B. X. Zhang¹, B. Y. Zhang^{1,43}, C. C. Zhang¹, D. H. Zhang¹, H. H. Zhang⁴⁴, H. Y. Zhang^{1,43}, J. Zhang^{1,47}, J. L. Zhang⁵⁹, J. Q. Zhang⁴, J. W. Zhang^{1,43,47}, J. Y. Zhang¹, J. Z. Zhang^{1,47}, K. Zhang^{1,47}, L. Zhang⁴⁵, T. J. Zhang^{38,h}, X. Y. Zhang³⁷, Y. Zhang^{53,43}, Y. H. Zhang^{1,43}, Y. T. Zhang^{53,43}, Yang Zhang¹, Yao Zhang¹, Yi Zhang^{9,j}, Z. H. Zhang⁶, Z. P. Zhang⁵³, Z. Y. Zhang⁵⁸, G. Zhao¹, J. W. Zhao^{1,43}, J. Y. Zhao^{1,47}, J. Z. Zhao^{1,43}, Lei Zhao^{53,43}, Ling Zhao¹, M. G. Zhao³⁴, Q. Zhao¹, S. J. Zhao⁶¹, T. C. Zhao¹, Y. B. Zhao^{1,43}, Z. G. Zhao^{53,43}, A. Zhemchugov^{27,b}, B. Zheng⁵⁴, J. P. Zheng^{1,43}, Y. H. Zheng⁴⁷, B. Zhong³², L. Zhou^{1,43}, Q. Zhou^{1,47}, X. Zhou⁵⁸, X. K. Zhou^{53,43}, X. R. Zhou^{53,43}, Xiaoyu Zhou²⁰, Xu Zhou²⁰, A. N. Zhu^{1,47}, J. Zhu³⁴, J. Zhu⁴⁴, K. Zhu¹, K. J. Zhu^{1,43,47}, S. H. Zhu⁵², W. J. Zhu³⁴, X. L. Zhu⁴⁵, Y. C. Zhu^{53,43}, Y. S. Zhu^{1,47}, Z. A. Zhu^{1,47}, J. Zhuang^{1,43}, B. S. Zou¹, J. H. Zou¹

(BESIII Collaboration)

¹ Institute of High Energy Physics, Beijing 100049, People's Republic of China² Beihang University, Beijing 100191, People's Republic of China³ Beijing Institute of Petrochemical Technology, Beijing 102617, People's Republic of China⁴ Bochum Ruhr-University, D-44780 Bochum, Germany⁵ Carnegie Mellon University, Pittsburgh, Pennsylvania 15213, USA⁶ Central China Normal University, Wuhan 430079, People's Republic of China⁷ China Center of Advanced Science and Technology, Beijing 100190, People's Republic of China

- ⁸ COMSATS Institute of Information Technology, Lahore, Defence Road, Off Raiwind Road, 54000 Lahore, Pakistan
- ⁹ Fudan University, Shanghai 200443, People's Republic of China
- ¹⁰ G.I. Budker Institute of Nuclear Physics SB RAS (BINP), Novosibirsk 630090, Russia
- ¹¹ GSI Helmholtzcentre for Heavy Ion Research GmbH, D-64291 Darmstadt, Germany
- ¹² Guangxi Normal University, Guilin 541004, People's Republic of China
- ¹³ Guangxi University, Nanning 530004, People's Republic of China
- ¹⁴ Hangzhou Normal University, Hangzhou 310036, People's Republic of China
- ¹⁵ Helmholtz Institute Mainz, Johann-Joachim-Becher-Weg 45, D-55099 Mainz, Germany
- ¹⁶ Henan Normal University, Xinxiang 453007, People's Republic of China
- ¹⁷ Henan University of Science and Technology, Luoyang 471003, People's Republic of China
- ¹⁸ Huangshan College, Huangshan 245000, People's Republic of China
- ¹⁹ Hunan Normal University, Changsha 410081, People's Republic of China
- ²⁰ Hunan University, Changsha 410082, People's Republic of China
- ²¹ Indian Institute of Technology Madras, Chennai 600036, India
- ²² Indiana University, Bloomington, Indiana 47405, USA
- ²³ (A)INFN Laboratori Nazionali di Frascati, I-00044, Frascati, Italy; (B)INFN and University of Perugia, I-06100, Perugia, Italy
- ²⁴ (A)INFN Sezione di Ferrara, I-44122, Ferrara, Italy; (B)University of Ferrara, I-44122, Ferrara, Italy
- ²⁵ Institute of Physics and Technology, Peace Ave. 54B, Ulaanbaatar 13330, Mongolia
- ²⁶ Johannes Gutenberg University of Mainz, Johann-Joachim-Becher-Weg 45, D-55099 Mainz, Germany
- ²⁷ Joint Institute for Nuclear Research, 141980 Dubna, Moscow region, Russia
- ²⁸ Justus-Liebig-Universität Giessen, II. Physikalisches Institut, Heinrich-Buff-Ring 16, D-35392 Giessen, Germany
- ²⁹ KVI-CART, University of Groningen, NL-9747 AA Groningen, The Netherlands
- ³⁰ Lanzhou University, Lanzhou 730000, People's Republic of China
- ³¹ Liaoning University, Shenyang 110036, People's Republic of China
- ³² Nanjing Normal University, Nanjing 210023, People's Republic of China
- ³³ Nanjing University, Nanjing 210093, People's Republic of China
- ³⁴ Nankai University, Tianjin 300071, People's Republic of China
- ³⁵ Peking University, Beijing 100871, People's Republic of China
- ³⁶ Seoul National University, Seoul, 151-747 Korea
- ³⁷ Shandong University, Jinan 250100, People's Republic of China
- ³⁸ Shanghai Jiao Tong University, Shanghai 200240, People's Republic of China
- ³⁹ Shanxi University, Taiyuan 030006, People's Republic of China
- ⁴⁰ Sichuan University, Chengdu 610064, People's Republic of China
- ⁴¹ Soochow University, Suzhou 215006, People's Republic of China
- ⁴² Southeast University, Nanjing 211100, People's Republic of China
- ⁴³ State Key Laboratory of Particle Detection and Electronics, Beijing 100049, Hefei 230026, People's Republic of China
- ⁴⁴ Sun Yat-Sen University, Guangzhou 510275, People's Republic of China
- ⁴⁵ Tsinghua University, Beijing 100084, People's Republic of China
- ⁴⁶ (A)Ankara University, 06100 Tandoğan, Ankara, Turkey; (B)Istanbul Bilgi University, 34060 Eyup, Istanbul, Turkey; (C)Uludağ University, 16059 Bursa, Turkey; (D)Near East University, Nicosia, North Cyprus, Mersin 10, Turkey
- ⁴⁷ University of Chinese Academy of Sciences, Beijing 100049, People's Republic of China
- ⁴⁸ University of Hawaii, Honolulu, Hawaii 96822, USA
- ⁴⁹ University of Jinan, Jinan 250022, People's Republic of China
- ⁵⁰ University of Minnesota, Minneapolis, Minnesota 55455, USA
- ⁵¹ University of Muenster, Wilhelm-Klemm-Str. 9, 48149 Muenster, Germany
- ⁵² University of Science and Technology Liaoning, Anshan 114051, People's Republic of China
- ⁵³ University of Science and Technology of China, Hefei 230026, People's Republic of China
- ⁵⁴ University of South China, Hengyang 421001, People's Republic of China
- ⁵⁵ University of the Punjab, Lahore-54590, Pakistan
- ⁵⁶ (A)University of Turin, I-10125, Turin, Italy; (B)University of Eastern Piedmont, I-15121, Alessandria, Italy; (C)INFN, I-10125, Turin, Italy
- ⁵⁷ Uppsala University, Box 516, SE-75120 Uppsala, Sweden
- ⁵⁸ Wuhan University, Wuhan 430072, People's Republic of China
- ⁵⁹ Xinyang Normal University, Xinyang 464000, People's Republic of China
- ⁶⁰ Zhejiang University, Hangzhou 310027, People's Republic of China
- ⁶¹ Zhengzhou University, Zhengzhou 450001, People's Republic of China
- ^a Also at Bogazici University, 34342 Istanbul, Turkey
- ^b Also at the Moscow Institute of Physics and Technology, Moscow 141700, Russia
- ^c Also at the Functional Electronics Laboratory, Tomsk State University, Tomsk, 634050, Russia
- ^d Also at the Novosibirsk State University, Novosibirsk, 630090, Russia
- ^e Also at the NRC "Kurchatov Institute", PNPI, 188300, Gatchina, Russia
- ^f Also at Istanbul Arel University, 34295 Istanbul, Turkey

^g Also at Goethe University Frankfurt, 60323 Frankfurt am Main, Germany

^h Also at Key Laboratory for Particle Physics, Astrophysics and Cosmology, Ministry of Education; Shanghai Key Laboratory for Particle Physics and Cosmology; Institute of Nuclear and Particle Physics, Shanghai 200240, People's Republic of China

ⁱ Government College Women University, Sialkot - 51310. Punjab, Pakistan.

^j Key Laboratory of Nuclear Physics and Ion-beam Application (MOE) and Institute of Modern Physics, Fudan University, Shanghai 200443, People's Republic of China

^k Currently at: Center for Underground Physics, Institute for Basic Science, Daejeon 34126, Korea

(Dated: November 2, 2018)

We report on the observation of the W -annihilation decay $D_s^+ \rightarrow \omega\pi^+$ and the evidence for $D_s^+ \rightarrow \omega K^+$ with a data sample corresponding to an integrated luminosity of 3.19 fb^{-1} collected with the BESIII detector at the center-of-mass energy $\sqrt{s} = 4.178 \text{ GeV}$. We obtain the branching fractions $\mathcal{B}(D_s^+ \rightarrow \omega\pi^+) = (1.77 \pm 0.32_{\text{stat.}} \pm 0.11_{\text{sys.}}) \times 10^{-3}$ and $\mathcal{B}(D_s^+ \rightarrow \omega K^+) = (0.87 \pm 0.24_{\text{stat.}} \pm 0.07_{\text{sys.}}) \times 10^{-3}$, respectively.

PACS numbers: 13.25.Ft, 12.38.Qk, 14.40.Lb

Within the Standard Model of particle physics, direct CP violation (CPV) in hadronic decays can only be induced in decays that proceed via at least two distinct decay amplitudes with non-trivial strong and weak phase differences [1–3]. In the charm sector, examples for such decays are the single Cabibbo suppressed (SCS) decays involving W -annihilation process [1–4], for example $D_s^+ \rightarrow \omega K^+$, and other VP final state (V and P refer to the vector and pseudo-scalar mesons, respectively). However, in D decays, the W -annihilation amplitude is dominated by the nonfactorizable long-distance amplitude induced by the final-state interaction (FSI). The corresponding theoretical calculation is very unreliable and results in some ambiguity in the prediction of the branching fractions (BFs) and the CPV of related decays. Instead, the experimental BF measurement of decays through the W -annihilation is used as an input in theoretical calculations [2–5]. Therefore, the BF of the Cabibbo favored (CF) decay $D_s^+ \rightarrow \omega\pi^+$ proceeding only via the W -annihilation process provides direct knowledge of the W -annihilation amplitude.

Compared with the SCS decays, the BF of $D_s^+ \rightarrow \omega\pi^+$ is expected to be larger and may be measured with a higher precision, is thus a more useful experimental input in the W -annihilation amplitude determination. Evidence for this decay was first reported by CLEO in 1997 and a ratio $\frac{\Gamma(D_s^+ \rightarrow \omega\pi^+)}{\Gamma(D_s^+ \rightarrow \eta\pi^+)} = 0.16 \pm 0.04 \pm 0.03$ was measured based on 4.7 fb^{-1} data taken at the $\Upsilon(4S)$ peak [6]. Later in 2009, using a data sample corresponding to an integrated luminosity of 0.586 fb^{-1} taken at center of mass energy $\sqrt{s} = 4.170 \text{ GeV}$, CLEO observed 6.0 ± 2.4 signal events and measured the absolute BF to be $(2.1 \pm 0.9) \times 10^{-3}$ [7].

With the previously measured W -annihilation $D \rightarrow VP$ decay as input, for $D_s^+ \rightarrow \omega K^+$, when considering the $\rho - \omega$ mixing, the BF and CPV are predicted to be

0.07×10^{-3} and -2.3×10^{-3} [3], respectively, where this predicted CPV is in the largest order of magnitude in charmed meson decays. However, the corresponding values are predicted to be 0.6×10^{-3} and -0.6×10^{-3} [3], respectively, when the $\rho - \omega$ mixing is negligible. Therefore, the search for $D_s^+ \rightarrow \omega K^+$ can also test the $\rho - \omega$ mixing effect and if $D_s^+ \rightarrow \omega K^+$ is a good decay mode to search for CPV in charm decays.

In this Letter, we report on measurements of the absolute BFs of the hadronic decays $D_s^+ \rightarrow \omega\pi^+$ and $D_s^+ \rightarrow \omega K^+$. Charge conjugation is implied throughout this Letter unless explicitly stated. At the center-of-mass energy of $\sqrt{s} = 4.178 \text{ GeV}$, the D_s^+ meson is predominantly produced through the process $e^+e^- \rightarrow D_s^{*+}D_s^- + c.c.$, where the D_s^{*+} decays to either γD_s^+ or $\pi^0 D_s^+$. As a consequence, any event that contains a D_s^+ meson also contains a D_s^- meson. This condition enables the usage of a powerful “double tag (DT)” technique [8] to measure absolute BFs. Events with at least one D_s^- candidate reconstructed, which are referred to as “single tag (ST)” events, provide a sample with a known number of $D_s^+D_s^-$ pairs. The absolute BF of the signal mode (\mathcal{B}_{sig}) is determined by forming DT signal events from the tracks and clusters not used to reconstruct the D_s^- candidate. The value of the BF can then be obtained using

$$\mathcal{B}_{\text{sig}} = \frac{Y_{\text{sig}}}{\sum_i \frac{Y_{\text{tag}}^i \epsilon_{\text{tag,sig}}^i}{\epsilon_{\text{tag}}^i}}, \quad (1)$$

where Y_{sig} is the DT signal yield, $\epsilon_{\text{tag,sig}}^i$ is the DT efficiency, and Y_{tag}^i and ϵ_{tag}^i are the ST yield and the ST efficiency of the i th tag mode, respectively.

A detailed description of the BESIII detector can be found in Ref. [9]. Two endcap time-of-flight systems were upgraded with multi-gap resistive plate chambers [10]. Monte Carlo (MC) simulations of BESIII detector are

based on GEANT4 [11]. The generic MC sample includes all known open charm processes, initial state radiation to the J/ψ or the $\psi(3686)$, and the continuum process. The open charm processes are generated with CONEXC [12], considering the effects from initial state radiation and final state radiation. The decay modes with known BFs are simulated with EVTGEN [13]. The generators KKMC [14] and BABAYAGA [15] are used to simulate the continuum. The generic MC sample, corresponding to an effective luminosity of 110.6fb^{-1} , is used to determine the ST efficiency and estimate the background. The signal MC sample, two million of events with one D_s meson decaying to the signal modes and the other one decaying to anything, as used in generic MC, is generated to estimate the DT efficiency.

ST and DT candidates are constructed from individual π^+ , K^+ , $K_S^0(\pi^+\pi^-)$ and $\pi^0/\eta(\gamma\gamma)$ candidates in an event. All charged tracks, except the K_S^0 daughters, are required to originate from within 10 cm (1 cm) along (perpendicular to) the beam axis with respect to the interaction point (IP). Their polar angles (θ) are required to be within $|\cos\theta| < 0.93$. The combination of information about the energy loss in the multi-layer drift chamber and the time-of-flight is used to identify the species of charged particles by calculating a probability $P(K^+)[P(\pi^+)]$ that the track satisfies the hypothesis of being a $K^+(\pi^+)$. The K^+ and π^+ candidates are required to satisfy $P(K^+) > P(\pi^+)$ and $P(\pi^+) > P(K^+)$, respectively.

For K_S^0 candidates, the combination of two oppositely charged tracks whose mass hypotheses are set to the pion, without particle identification (PID) applied and with distances of closest approach to the IP less than 20 cm along the beam axis, is required to have an invariant mass in the interval $[0.487, 0.511]\text{ GeV}/c^2$.

The energy of each photon from the π^0/η is required to be larger than 25 (50) MeV in the barrel (endcap) region of the electromagnetic calorimeter [9]. The opening angles between the shower and all the charged tracks should be larger than 10° . The invariant mass of the $\gamma\gamma$ pair is required to be within the asymmetric intervals $[0.115, 0.150]$ and $[0.490, 0.580]\text{ GeV}/c^2$ for π^0 and η . Furthermore, the π^0/η candidates are constrained to their nominal mass [16] via a kinematic fit to improve their energy and momentum resolution.

The momenta of all pions, except those from the decay of K_S^0 , are required to be greater than $0.1\text{ GeV}/c$ in order to reject low momentum pions produced in the D^* decay. The ST events are selected by reconstructing a D_s^- meson in the two highest purity decay modes $D_s^- \rightarrow K_S^0 K^-$ and $K^+ K^- \pi^-$. For the D_s candidate, a recoil mass M_{rec} is defined as $M_{\text{rec}} = \sqrt{(E_{\text{tot}} - \sqrt{p_{D_s}^2 + m_{D_s}^2})^2 - |\vec{p}_{\text{tot}} - \vec{p}_{D_s}|^2}$, where

E_{tot} , p_{D_s} , m_{D_s} , \vec{p}_{tot} and \vec{p}_{D_s} are the total energy of e^+e^- , the momentum of the D_s candidate, the nominal mass of D_s [16], the three-momentum vector of the colliding e^+e^- system, and the three-momentum vector of the reconstructed D_s candidate, respectively. If the selected D_s^- candidate originates directly from the e^+e^- annihilation, M_{rec} peaks at the D_s^* mass ($m_{D_s^*}$). The other D_s candidate has a broader distribution around $m_{D_s^*}$ in the M_{rec} spectrum. The D_s invariant mass and M_{rec} of the candidate are required to fall into the ranges $[1.90, 2.03]\text{ GeV}/c^2$ and $[2.05, 2.18]\text{ GeV}/c^2$, respectively. If there are multiple candidates in an event, the one with M_{rec} closest to $m_{D_s^*}$ [16] is chosen.

The ST yields are extracted from fits to the invariant mass spectra (M_{tag}) of the ST D_s^- candidates, the results are shown in Fig. 1. The signal shape is modeled as a double Gaussian, while the background is parameterized as a second-order Chebychev polynomial. The

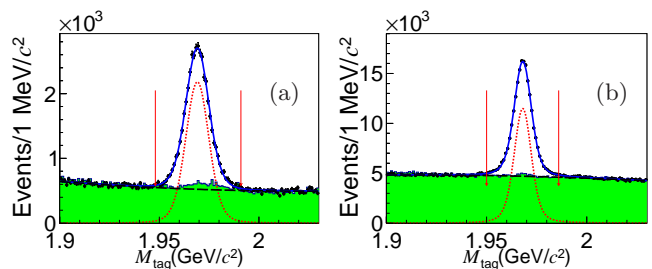


FIG. 1. Fits to the M_{tag} spectra of (a) $D_s^+ \rightarrow K_S^0 K^+$ and (b) $D_s^+ \rightarrow K^- K^+ \pi^+$. The dots with error bars are data, the solid lines are the total fits, the dashed lines and the dotted lines are the shapes of signal and fitted background, respectively. The (green) filled histograms are the MC-simulated backgrounds. The D_s signal regions are between the arrows.

signal regions are defined as: $[1.948, 1.991]\text{ GeV}/c^2$ for $D_s^- \rightarrow K_S^0 K^-$ and $[1.950, 1.986]\text{ GeV}/c^2$ for $D_s^- \rightarrow K^+ K^- \pi^-$, respectively. The ST yields determined by the fit for $D_s^- \rightarrow K_S^0 K^-$ and $D_s^- \rightarrow K^+ K^- \pi^-$ are 32751 ± 313 and 131862 ± 773 , respectively. For the tag mode $D_s^- \rightarrow K_S^0 K^-$, a small peak in the background is observed in the signal region; this is due to $D^- \rightarrow K_S^0 \pi^-$ events with the π^- misidentified as a K^- . From the generic MC sample, the yield of the $D^- \rightarrow K_S^0 \pi^-$ background is estimated to be around 250, corresponding to about 0.2% of the total ST yields, which is considered in the systematic uncertainty. For the tag mode $D_s^- \rightarrow K^+ K^- \pi^-$, a much smaller bump can also be found and the effect is negligible.

The DT events are reconstructed $D_s^+ D_s^-$ pairs with D_s^- reconstructed in a tag mode combined with $D_s^+ \rightarrow \omega \pi^+$ or $D_s^+ \rightarrow \omega K^+$ candidates, in which the ω is reconstructed in the $\pi^+ \pi^- \pi^0$ final state. For the two D_s candidates, we require that at least one of them has M_{rec} greater than $2.10\text{ GeV}/c^2$. If there is more than one

$D_s^+ D_s^-$ pair candidate, the one with an average invariant mass of the two D_s mesons closest to m_{D_s} is chosen.

For $D_s^+ \rightarrow \omega K^+$, the background from the decay $D_s^+ \rightarrow K_S^0 K^+ \pi^0$ is identical to the signal in the M_{rec} distribution and forms a peak around the $K^*(892)$ mass in the $\pi^+ \pi^- \pi^0$ invariant mass ($M_{\pi^+ \pi^- \pi^0}$) spectrum. Consequently, we further perform a K_S^0 veto to suppress this background. If the invariant mass of the $\pi^+ \pi^-$ ($M_{\pi\pi}$) combination in $D_s^+ \rightarrow \omega K^+$ signal candidate satisfies $|M_{\pi\pi} - m_{K_S^0}| < 0.03 \text{ GeV}/c^2$ and the distance between the decay point and the IP has a significance of more than two standard deviations, the events are vetoed. This veto eliminates about 78% of $D_s^+ \rightarrow K_S^0 K^+ \pi^0$ background, while retaining about 97% of signal events. After the K_S^0 veto, this background is found to be negligible according to the generic MC.

A two dimensional (2D) extended unbinned likelihood fit is performed to the $M_{\pi^+ \pi^- \pi^0}$ and the signal D_s invariant mass (M_{sig}) distributions to extract the signal yield. For $D_s^+ \rightarrow \omega \pi^+$ candidates, there are two $\pi^+ \pi^- \pi^0$ combinations formed in each event. In the data sample, there are 5 events with both $\pi^+ \pi^- \pi^0$ combinations retained in the fit range of $[0.60, 0.95] \text{ GeV}/c^2$, but there is no evidence that these events create a peak. This effect is negligible in the fit.

The D_s signal is described by the MC simulated signal shape convolved with a Gaussian ($f_{D_s}^{\text{peak}}$). Here, the mean and the resolution of the Gaussian are fixed at the values determined from the fit to the sample of $D_s^+ \rightarrow \pi^+ \pi^- \pi^0 \pi^+ (K^+)$ in data. The ω signal is represented by a Breit-Wigner (BW) convolved with a Gaussian (f_{ω}^{peak}), where the mass and width are fixed to the PDG values [16]. The resolution of the Gaussian is fixed at the value determined from the sample of $e^+ e^- \rightarrow K^+ K^- \omega$. The combinatorial background in M_{sig} and $M_{\pi^+ \pi^- \pi^0}$ spectra are parameterized by second-order Chebychev polynomials ($f_{D_s}^{\text{poly}}$ and f_{ω}^{poly}).

The scatter plots of M_{sig} versus $M_{\pi^+ \pi^- \pi^0}$ for the two signal decays are shown in Figs. 2(a,b), from which no obvious correlation between M_{sig} and $M_{\pi^+ \pi^- \pi^0}$ is found, which is also confirmed by signal MC. The 2D fit model is then constructed as following. The signal shape is modeled as the product of $f_{D_s}^{\text{peak}}$ and f_{ω}^{peak} . The background that does not peak in both $M_{\pi^+ \pi^- \pi^0}$ and M_{sig} distributions (BKGI) is modeled as the product of $f_{D_s}^{\text{poly}}$ and f_{ω}^{poly} . The background with an ω that peaks in the $M_{\pi^+ \pi^- \pi^0}$ distribution (BKGII) is modeled as the product of $f_{D_s}^{\text{poly}}$ and f_{ω}^{peak} . The background from $D_s^+ \rightarrow \pi^+ \pi^- \pi^0 \pi^+ (K^+)$ that only has a peak in the M_{sig} distribution (BKGIII) is modeled as the product of $f_{D_s}^{\text{peak}}$ and f_{ω}^{poly} . The parameters in $f_{D_s}^{\text{poly}}$ and f_{ω}^{poly} obtained in the individual fits to the M_{sig} and $M_{\pi^+ \pi^- \pi^0}$ spectra, respectively. Therefore, in the 2D fit, yields of signal and

backgrounds are determined by the fit and the other parameters are fixed at the values from the individual fits. From the 2D fits, we obtain $65.0 \pm 11.6 D_s^+ \rightarrow \omega \pi^+$ signals and $28.5 \pm 7.8 D_s^+ \rightarrow \omega K^+$ signals with statistical significances of 6.7σ and 4.4σ , respectively. The fit results are shown in Figs. 2(b,c,e,f).

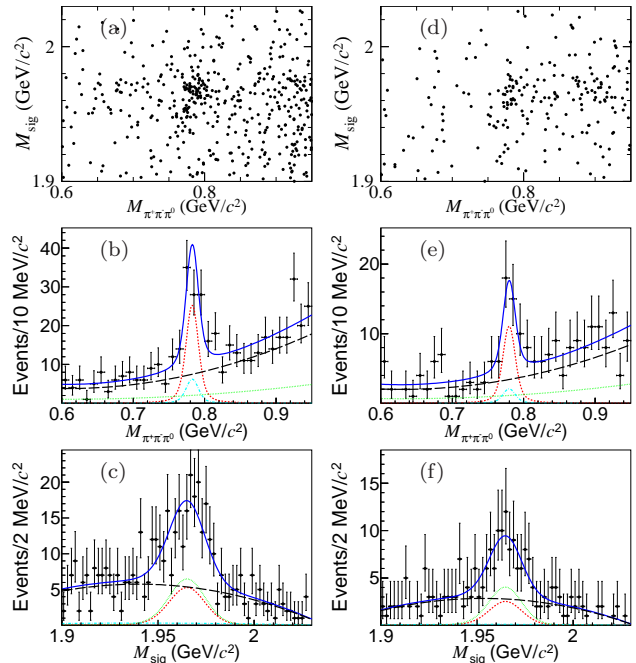


FIG. 2. The ((a) and (d)) scatter plots of M_{sig} versus $M_{\pi^+ \pi^- \pi^0}$, fit results of ((b) and (e)) $M_{\pi^+ \pi^- \pi^0}$, and fit results of ((c) and (f)) M_{sig} for (a-c) $D_s^+ \rightarrow \omega \pi^+$ and (d-f) $D_s^+ \rightarrow \omega K^+$. In the fits, the dots with error bars are data, the (blue) solid lines describe the total fits, the (red) dashed lines describe the signal shape and the (green) dotted, (cyan) dash-dotted, and (black) long dashed lines describe the BKGI, BKGII, and BKGIII, respectively.

The ST and DT efficiencies are determined from the generic MC and signal MC samples, respectively. All efficiencies are summarized in Table I. Using Eq. (1) and the

TABLE I. The ST efficiencies ϵ_{tag} and DT efficiencies $\epsilon_{\text{tag, sig}}$.

Tag mode	ϵ_{tag} (%)	$\epsilon_{\text{tag, } \omega \pi^+}$ (%)	$\epsilon_{\text{tag, } \omega K^+}$ (%)
$D_s^- \rightarrow K_S^0 (\pi^+ \pi^-) K^-$	51.38 ± 0.25	12.53 ± 0.13	10.74 ± 0.11
$D_s^- \rightarrow K^+ K^- \pi^-$	38.44 ± 0.08	9.79 ± 0.06	8.81 ± 0.06

world averaged BF's of $\omega \rightarrow \pi^+ \pi^- \pi^0$ and $\pi^0 \rightarrow \gamma \gamma$ [16], the BF's are measured to be: $\mathcal{B}(D_s^+ \rightarrow \omega \pi^+) = (1.77 \pm 0.32) \times 10^{-3}$ and $\mathcal{B}(D_s^+ \rightarrow \omega K^+) = (0.87 \pm 0.24) \times 10^{-3}$, where the uncertainties are statistical.

The systematic uncertainties are investigated and are summarized in Table II. For each decay, the total systematic uncertainty is obtained by adding the individual

terms in quadrature.

The uncertainties due to the M_{rec} requirement and momentum requirement on pion are estimated with the control sample of $D_s^+ \rightarrow \pi^+\pi^-\pi^+\eta$, with η' decays removed by requiring the invariant mass of $\pi^+\pi^-\eta$ to be greater than $1.0 \text{ GeV}/c^2$. The uncertainty due to the K_S^0 veto is estimated with the control sample of $D^0 \rightarrow K_S^0\omega$. The differences between the efficiencies caused by corresponding selection criterion obtained from data and MC simulation are taken as the systematic uncertainties.

The uncertainties for charged tracks selection are determined to be 0.5%/track for PID and 1.0%/track for tracking using the control sample of $e^+e^- \rightarrow K^+K^-\pi^+\pi^-$. The uncertainty of the π^0 reconstruction efficiency is investigated with the control sample of $e^+e^- \rightarrow K^+K^-\pi^+\pi^-\pi^0$, and is determined to be 1.8% (1.9%) for $D_s^+ \rightarrow \omega\pi^+(K^+)$. The uncertainty due to the MC statistics is 0.6%.

The uncertainty due to the signal shape is estimated by varying the masses and resolutions of the ω and D_s within their uncertainties. The uncertainty due to the background shape is investigated by narrowing the fit ranges of $M_{\pi^+\pi^-\pi^0}$ and M_{sig} to $[0.65, 0.90] \text{ GeV}/c^2$ and $[1.91, 2.02] \text{ GeV}/c^2$, respectively, and replacing the second-order Chebychev polynomial in $f_{D_s^+}^{\text{poly}}$ and f_{ω}^{poly} by a first-order Chebychev polynomial. The uncertainty related to ST yields is estimated using the MC-simulated shape to replace the Gaussian function in the ST yields determination. Here, the effect from the bump under the $D_s^- \rightarrow K_S^0K^-$ signal region is also taken into account. For each alteration of the fit configuration the measurements are re-performed. The largest change to the BF is taken as the corresponding uncertainty. The uncertainty from the shape and fit ranges effect of background in ST yields is found to be negligible. The uncertainty due to the fit procedure is investigated by studying ten statistically independent samples of generic MC events with the same size as data. With the same method as used in data analysis, the average measured BF is found to have a relative difference of 0.8% with respect to the input value. This difference is taken as the uncertainty from the fit procedure. The uncertainty related to the assumed BFs for $\omega \rightarrow \pi^+\pi^-\pi^0$ and $\pi^0 \rightarrow \gamma\gamma$ is taken from the PDG [16].

In summary, we observe the W -annihilation decay $D_s^+ \rightarrow \omega\pi^+$ with a significance of 6.7σ and measure its BF to be $(1.77 \pm 0.32_{\text{stat.}} \pm 0.12_{\text{sys.}}) \times 10^{-3}$. This measurement provides critical information to determine the non-perturbative W -annihilation amplitudes. The significantly improved precision benefits the investigations of the underlying dynamics in charmed hadronic decays, and will allow better predictions for the BFs and direct CPV of decays involving W -annihilation [1, 3–5]. Among these decays, $D_s^+ \rightarrow \omega K^+$ is interest for its

TABLE II. Relative systematic uncertainties (%) in the BF measurements.

Source	$D_s^+ \rightarrow \omega\pi^+$	$D_s^+ \rightarrow \omega K^+$
M_{rec} requirement	0.1	
Momentum requirement on pion	1.7	
K_S^0 veto	-	0.1
PID of K^\pm, π^\pm	1.5	1.5
Tracking of K^\pm, π^\pm	3.0	3.0
π^0 reconstruction	1.8	1.9
MC statistics	0.6	0.6
Background shape	4.1	4.6
Signal shape	3.3	5.3
ST yield	1.3	1.3
Fit procedure	0.8	
$\mathcal{B}(\omega \rightarrow \pi^+\pi^-\pi^0)$ & $\mathcal{B}(\pi^0 \rightarrow \gamma\gamma)$	0.8	
Total	7.0	8.4

possibly large CPV. We find the first evidence for this decay with a significance of 4.4σ . Its BF is measured to be $(0.87 \pm 0.24_{\text{stat.}} \pm 0.07_{\text{sys.}}) \times 10^{-3}$. According to Ref. [3], our result implies that the $\rho - \omega$ mixing is negligible and direct CP asymmetry is expected at the level of -0.6×10^{-3} .

The authors wish to thank Fusheng Yu for useful discussions. The BESIII collaboration thanks the staff of BEPCII and the IHEP computing center for their strong support. This work is supported in part by National Key Basic Research Program of China under Contract No. 2015CB856700; National Natural Science Foundation of China (NSFC) under Contracts Nos. 11425524, 11625523, 11635010; the Chinese Academy of Sciences (CAS) Large-Scale Scientific Facility Program; the CAS Center for Excellence in Particle Physics (CCEPP); Joint Large-Scale Scientific Facility Funds of the NSFC and CAS under Contracts Nos. U1332201, U1532257, U1532258; CAS Key Research Program of Frontier Sciences under Contracts Nos. QYZDJ-SSW-SLH003, QYZDJ-SSW-SLH040; 100 Talents Program of CAS; National 1000 Talents Program of China; INPAC and Shanghai Key Laboratory for Particle Physics and Cosmology; German Research Foundation DFG under Contracts Nos. Collaborative Research Center CRC 1044, FOR 2359; Istituto Nazionale di Fisica Nucleare, Italy; Koninklijke Nederlandse Akademie van Wetenschappen (KNAW) under Contract No. 530-4CDP03; Ministry of Development of Turkey under Contract No. DPT2006K-120470; National Science and Technology fund; The Swedish Research Council; U. S. Department of Energy under Contracts Nos. DE-FG02-05ER41374, DE-SC-0010118, DE-SC-0010504, DE-SC-0012069; University of Groningen (RuG) and the Helmholtzzentrum fuer Schwerionenforschung GmbH (GSI), Darmstadt; WCU Program of National Research Foundation of Korea under Contract No. R32-2008-000-10155-0.

-
- [1] H. Y. Cheng and C. W. Chiang, Phys. Rev. D **85**, 034036 (2012); Erratum: [Phys. Rev. D **85**, 079903 (2012)].
- [2] H. n. Li, C. D. Lu and F. S. Yu, Phys. Rev. D **86**, 036012 (2012).
- [3] Q. Qin, H. N. Li, C. D. Lü and F. S. Yu, Phys. Rev. D **89**, 054006 (2014).
- [4] H. Y. Cheng and C. W. Chiang, Phys. Rev. D **81**, 074021 (2010).
- [5] H. Y. Cheng, C. W. Chiang and A. L. Kuo, Phys. Rev. D **93**, 114010 (2016).
- [6] R. Balest *et al.* (CLEO Collaboration), Phys. Rev. Lett. **79**, 1436 (1997).
- [7] J. Y. Ge *et al.* (CLEO Collaboration), Phys. Rev. D **80**, 051102(R) (2009).
- [8] R. M. Baltrusaitis *et al.* (Mark III Collaboration), Phys. Rev. Lett. **56**, 2140 (1986).
- [9] M. Ablikim *et al.* (BESIII Collaboration), Nucl. Instrum. Methods Phys. Res., Sect. A **614**, 345 (2010).
- [10] X. Wang *et al.*, JINST **11**, no. 08, C08009 (2016).
- [11] S. Agostinelli *et al.* (GEANT4 Collaboration), Nucl. Instrum. Methods Phys. Res., Sect. A **506**, 250 (2003).
- [12] R. G. Ping, Chin. Phys. C **38**, 083001 (2014).
- [13] D. J. Lange, Nucl. Instrum. Methods Phys. Res., Sect. A **462**, 152 (2001); R. G. Ping, Chin. Phys. C **32**, 599 (2008).
- [14] S. Jadach, B. F. L. Ward and Z. Was, Phys. Rev. D **63**, 113009 (2001).
- [15] C. M. Carloni Calame *et al.*, Nucl. Phys. B (Proc. Suppl.) **131**, 48 (2004).
- [16] M. Tanabashi *et al.* (Particle Data Group), Phys. Rev. D **98**, 030001 (2018).
- [17] M. Ablikim *et al.* (BESIII Collaboration), Phys. Rev. Lett. **116**, 082001 (2016).